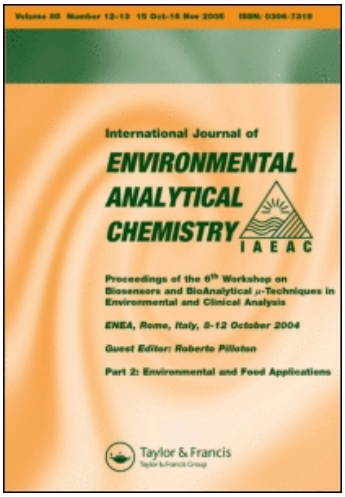

International Journal of Environmental Analytical Chemistry
Publication details, including instructions for authors and subscription information:
http://www.informaworld.com/smpp/title~content=t713640455

^{1}H-NMR Micro-Imaging and Correlated Sem Studies of Spruce Needles from Healthy and Declined Forest Sites

Georg Masuch[a]; Jörg Thomas Franz[a]; Heinrich Marsmann[b]; Dieter Groβ[c]; Antonius Kettrup[d]
[a] Angewandte Botanik, Universität-GH Paderborn, Paderborn, Germany [b] Anorganische Chemie, Universität-GH Paderborn, Paderborn, Germany [c] Bruker Analytische Meβtechnik GmbH, Rheinstetten, Germany [d] GSF—, Forschungszentrum für Umwelt und Gesundheit Institut für Ökologische Chemie, München, Neuherberg, Germany

To cite this Article Masuch, Georg , Franz, Jörg Thomas , Marsmann, Heinrich , Groβ, Dieter and Kettrup, Antonius(1991) '^{1}H-NMR Micro-Imaging and Correlated Sem Studies of Spruce Needles from Healthy and Declined Forest Sites', International Journal of Environmental Analytical Chemistry, 45: 3, 179 — 191
To link to this Article: DOI: 10.1080/03067319108026989
URL: http://dx.doi.org/10.1080/03067319108026989

Intern. J. Environ. Anal. Chem., Vol. 45, pp. 179–191
Reprints available directly from the publisher
Photocopying permitted by license only

^{1}H-NMR MICRO-IMAGING AND CORRELATED SEM STUDIES OF SPRUCE NEEDLES FROM HEALTHY AND DECLINED FOREST SITES

GEORG MASUCH and JÖRG-THOMAS FRANZ

Angewandte Botanik, Universität-GH Paderborn, Warburgerstr. 100, D-4790 Paderborn, Germany.

HEINRICH MARSMANN

Anorganische Chemie, Universität-GH Paderborn, Warburgerstr. 100, D-4790 Paderborn, Germany.

DIETER GROß

Bruker Analytische Meßtechnik GmbH, D-7512 Rheinstetten, Germany.

and

ANTONIUS KETTRUP

GSF—Forschungszentrum für Umwelt und Gesundheit Institut für Ökologische Chemie, D-8042 München-Neuherberg, Germany.

(Received 20 July 1990; in final form 20 June 1991)

^{1}H-NMR micro-imaging is a technique for measuring mobile proton density and for obtaining cross-sectional pictures of quantitative distribution of water in living tissues. An application comparing healthy and damaged Norway spruce needles of a slightly polluted stand of the Sauerland area, Germany, and a severely polluted stand of the Eggegebirge, Germany, is presented. Damaged needles show a higher proton signal intensity and a different distribution of free water in the needle tissues compared with healthy needles. ^{1}H-NMR microimaging and correlated SEM studies give rise to an integrated interpretation of symptoms caused by air pollution.

KEY WORDS: ^{1}-NMR micro-imaging, tissue water distribution, nondestructive analysis, Norway spruce needle, *Picea abies Karst.*, forest decline.

INTRODUCTION

The first use of magnetic field gradients to measure nuclear spin densities by nuclear magnetic resonance (NMR) started in the early 1970s[1,2]. Nuclear magnetic resonance imaging employs the spational dependence of nuclear Larmor frequencies in the presence of allied magnetic field gradients to determine nuclear position. Protons have the greatest Larmor frequency among stable nuclei and therefore provide the greatest sensitivity. In biological tissue, the most abundent source of ^{1}H nuclei

is the water molecule and in most cases proton density may be equated with water density in NMR imaging[3]. Pulsed NMR techniques were used to measure moisture content of white spruce in the moisture content range from 0 to 176%[4]. Recently it has been shown that NMR imaging may be used on a microscopic scale to image water distribution in plant stems[5]. Microscopic imaging differs from its large-scale counterpart in the need for larger magnetic field gradients. It is the loss of signal consequent on reducing the voxel size which ultimately limits the resolution[6] available in a given imaging time. On our system, operating at 300 MHz, we have achieved a pixel resolution of 11 μm in a slice 990 μm thick. Proton images display the total mobile proton density reflecting predominantly the water distribution.

The aim of ^{1}H-NMR micro-imaging technique is to measure mobile proton density as a function of position and to display this information suitably encoded as an image. Thus, a physiological interpretation based on the correlated anatomical structures in facilitated.

An important application of such a correlated methodical action is the investigation of forest die-back. The phenomenon of forest decline is characterized by a variety of growth-decreasing, abnormal-growth and water-stress symptoms[7]. Evidence suggests that physiological disturbances in plant water relation induced by air pollutants may have contributed to forest decline in both Europe and North America[8].

Pollutants may influence water loss through the leaves and changes in the water relations of cells and tissues. Cellular water relations are usually investigated using pressure-volume analysis[9,10,11]. In the positron-emission-transversal tomography (PETT) short-lived isotopes are used, e.g. $H_2{}^{15}O$ for estimating water content[12]. One advantage of ^{1}H-NMR micro-imaging is the fact that cross-sectional pictures through living organs can be obtained without exposing the living tissue to ionizing radiation and without damaging living cvells.

The present investigation was undertaken to compare the water distribution measured by ^{1}H-NMR micro-imaging and the histological condition of spruce needles from a declined forest stand and a healthy forest stand. The final objective of this study is to investigate whether ^{1}H-NMR micro-imaging is a useful technique to discriminate sensitively between healthy and diseased needle tissues.

EXPERIMENTAL

Research stands of Velmerstot and Glindfeld

The Egge Mountains and the forest stand of Velmerstot within it have become the main forest decline stand in Northrhine Westphalia; in 1988 forest decline has reached an average percentage of 49.8%. The forest stands of the Sauerland and the forest district Glindfeld within it are less injured (34.4%).

Second-year needle samples of Norway spruces (*Picea abies Karst.*) were taken from three trees (41 years old) of the research stand of Velmerstot and from three trees (48 years old) of the research stand of Glindfeld in November 1989.

In accordance with the standardised guidelines drawn up in the framework of the United Nations' Economic Commission for Europe (UN-ECE), the selected trees of

the Glindfeld stand belong to the healthy class (damage category 0) or to the slightly injured class (damage category 1). The selected trees of the Velmerstot stand belong to the severely injured class (damage category 3). The average air pollution concentrations for the Velmerstot stand in 1989 (1988) were 20.2 (38) $\mu g/m^3$ SO_2, 18.5 (21) $\mu g/m^3$ NO_2, 69 (57) $\mu g/m^3$ O_3; those for the Glindfeld stand were 13.5 (13) $\mu g/m^3$ SO_2, 15.8 (20) $\mu g/m^3$ NO_2, 67.5 (64) $\mu g/m^3$ O_3 [13]. For further ecological data, one should consult ref. 14.

NMR Micro-imaging

NMR micro-imaging was used to detect the distribution of water in spruce needles. The experiments were performed on a Bruker AM 300 spectrometer, operating at 300 MHz (1H), equipped with microscopy hardware and software and a 7 T vertical bore superconducting magnet. The proton signal was picked up by a solenoid coil of 3 mm diameter and 15 mm length. Several spruce needles can be placed inside the coil at the same time, so that differences between healthy and damaged needles are visualized in one single experiment under the same experimental conditions. The whole spruce needles were put into a glass tube with sealed ends to prevent water loss during the experiment. 256*256 pixel images were measured by the single splice spin echo method[15] and reconstructed with the two-dimensional Fourier transformation method. The proton spins were excited by a 90° pulse of 4 μs length and refocused by a 2 ms hermitian shaped pulse. In order to collect the signals from all water protons, even from those with rather short spin-spin relaxation times, the spin echo time, TE, was kept short (TE = 7.4 ms), using a spectral width of 50 kHz and gradient switching times of 300 μs. A real gradient strength of 400 mT/m and a slice select gradient of 33 mT/m resulted in a resolution of 11 μm/pixel and a slice thickness of 990 μm.

Biological methods

Preparation and fixation methods of spruce needles are reported in an earlier paper[16]. Preparation of needles for qualitative histological investigation was carried out on identical needles after having finished off ^{1}H-NMR micro-imaging. Amyl-acetate was used as a solvent to extract resin from semi-thin sections for SEM observation. Specimens were the dried, mounted and coated with gold by sputtering. Quantitative analysis of tissues was made from 10 light microscopic pictures per stand, photographed from specimens of different needles. A digitizer tablet, connected to a micro-computer was used for tissue area measuring. Electron microscopic studies were performed with a Hitachi H 3010 scanning electron microscope. For observation of epicuticular waxes needles were removed with forceps, vacuum-dried and affixed to aluminium stubs coated with gold by sputtering for SEM.

RESULTS

Histological changes

In the quantitative approach to the histological analysis spruce needles revealed differences between healthy and injured forest sites (Figures 1 and 2).

In the transverse section of second-year needles the following tissue parameters of the Velmerstot stand significantly decrease in their transverse section areas relative to those of the Glindfeld stand: the needle transverse section area, the mesophyll cell area, the intercellular space area and the vascular bundle area (Figures 1, 2 and 3).

The decrease of the transverse section area of the mesophyll cell tissue is due to a reduced amount of mesophyll cells. The average mesophyll cell number in needle transverse sections of the healthy site (Glindfeld) is 288 $\pm$ 16: that of the injured site (Velmerstot) is 226 $\pm$ 15 ($P = 0$). No significant difference could be found in the average size of mesophyll cells. The mean needle length of the injured spruces of the Velmerstot stand was significantly longer (19.5 $\pm$ 0.6 mm) than that of the healthy Glindfeld stand (15.8 $\pm$ 0.5 mm; $P = 0$). The external surface areas of Velmerstot

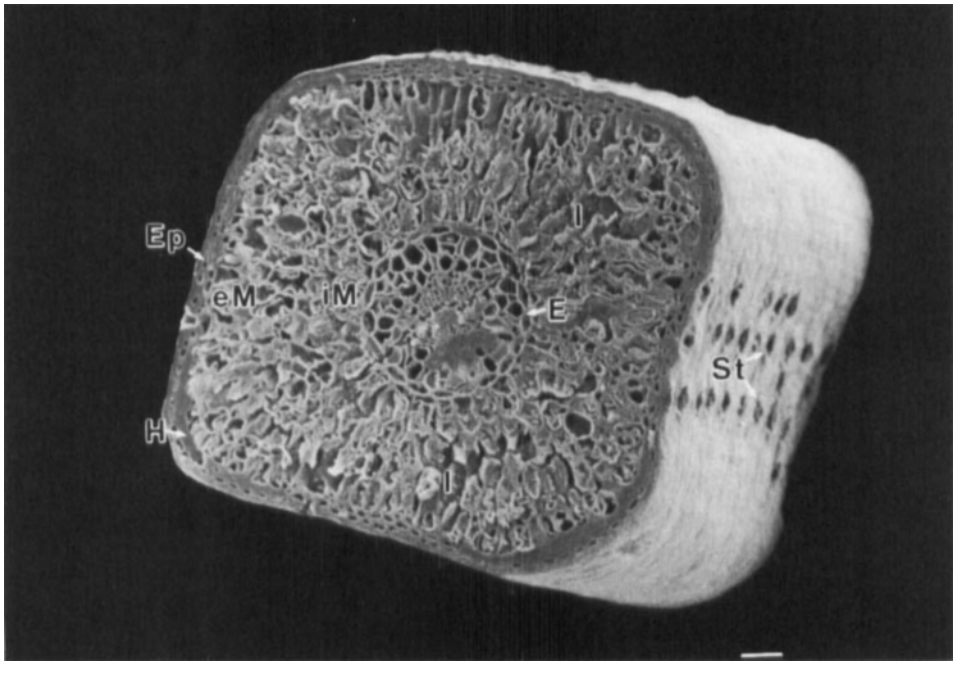

Figure 1 Transverse section of a second year Norway spruce needle of a healthy forest site (Glindfeld). This SEM picture and the ^{1}H-NMR images in the upper right of the Figures 10 and 11 come from the identical spruce needle. Bar = 50 μm. The following tissues are marked off: E, endodermis; Ep, epidermis; H, hypodermis; I, intercellular space; eM, external part of mesophyll tissue; iM, internal part of mesophyll tissue; St, stomatal rows.

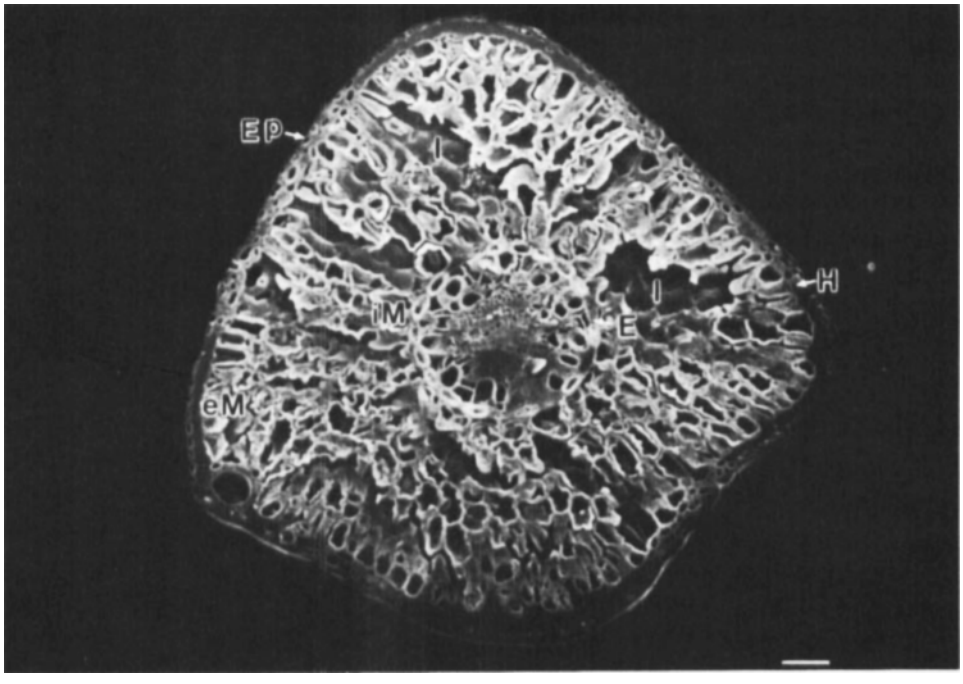

Figure 2 Transverse section of a second year Norway spruce needle of an injured forest site (Velmerstot). This SEM picture and the ^{1}H-NMR images in the lower left of the Figures 10 and 11 come from the identical spruce needle. Bar = 50 μm. Explanations of abbreviations see legend of Figure 1.

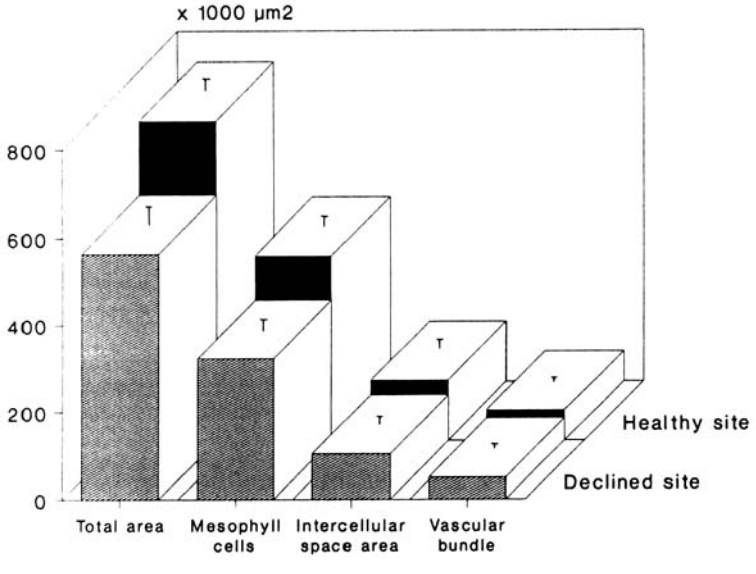

Figure 3 Tissue areas of transverse sections of second year Norway spruce needles of a healthy forest site (Glindfeld) and a declined forest site (Velmerstot) (P = 0).

needles had significantly ($P = 0$) increased ($57 \pm 1.8\ mm^2$) relative to those of the Glindfeld stand ($52 \pm 1.5\ mm^2$). The number of stomates per $1\ mm^3$ intercellular space volume was higher in injured needles of the Velmerstot stand ($968 \pm 75\ mm^3$ intercellular space) than in the healthy ones of the Glindfeld stand ($829 \pm 140\ mm^3$; $P = 0.08$). Still, the tissue volume of the total needle had decreased as mentioned above for the transverse section areas. Concerning the vascular bundle the most conspicuous changes occur in the transfusion tissues, that are reduced by 31% in the injured needles, followed by the xylem tissue which are reduced by 20%. There is no difference in the phloem tissue area between needles of the two sites, but intact sieve elements can be found more frequently in transverse sections of needles of the healthy site in Glindfeld (Figure 4). Main phloem parts of needles of the injured site are collapsed and out of function (Figure 5).

Needle wax degradation

The structure of epistomatal and non-stomatal waxes of second-year needle surfaces show remarkable differences between spruces of the Glindfeld site and the Velmerstot site.

Needles from trees growing in healthy or slightly polluted atmospheres of the Glindfeld stand show highly structured surface waxes (Figure 6). Wax structures protrude from the surface of the guard cells and subsidary cells of the epistomatal chambers (Figure 7) and from the surface of epidermal cells in non-stomatal areas.

Spruce needles of the polluted forest stand (Velmerstot) show faster weathering and fusion of wax fibrils (Figures 8 and 9). Extremely rapid wax erosion and formation of a wax layer is obvious (Figure 9). It cannot be excluded that cracks in the wax layer (Figure 8) may occur during specimen preparation.

Water distribution in needle tissues

The distribution of water quantities in healthy and injured needles is quite different. Figures 10 and 11 show representative proton spin-echo NMR images of spruce needles using a spin-echo time of 7.4 ms. The figures demonstrate the distribution of the signal intensity in the cross-section.

Generally it can be said that second-year needles of the injured site (Velmerstot) contain more water than those of the healthy site (Glindfeld). This information has also been achieved by gravimetrical methods. As measured in July 1988 the relative water content of second-year needles of the healthy Glindfeld stand was found to be 47.7% of fresh weight (mean of three samples of different trees); second-year needles from the severely polluted Velmerstot stand showed an increased relative water content of 55.7% of fresh weight.

Concerning the healthy needles of the Glindfeld stand, the highest signal intensities come from the endodermis, the peripheral part of the mesophyll tissue and parts of the vascular bundle. In contrast to the external part of the mesophyll tissue, the internal part shows very little signal. This implies that the internal mesophyll tissue contains lower amounts of free water than the external mesophyll tissues. As

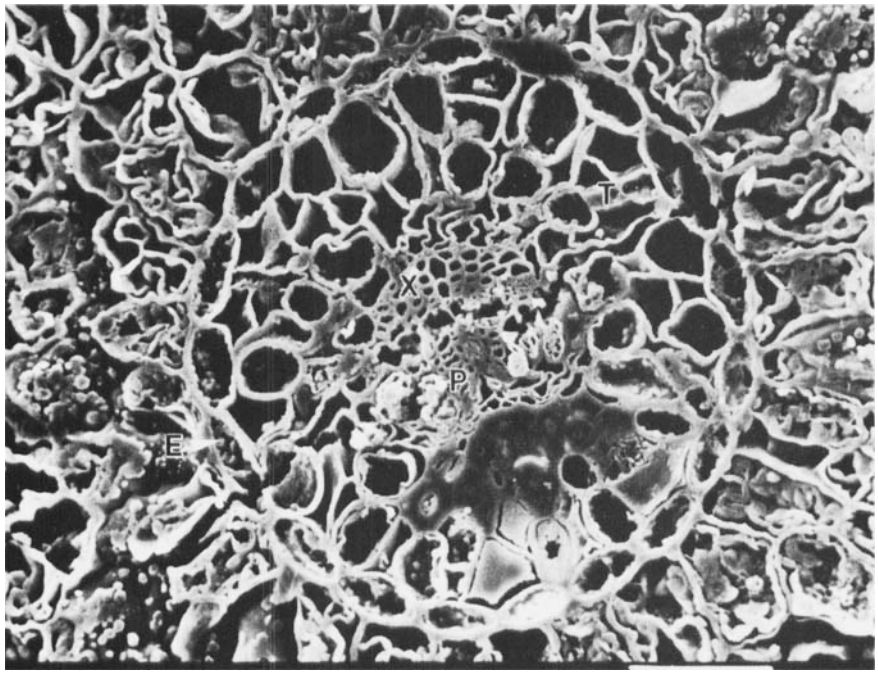

Figure 4 Transverse section of a vascular bundle of a second year Norway spruce needle of the healthy forest site of Glindfeld (enlarged detail from identical needle of Figure 1). Bar = 50 μm. The following tissues are marked off: E, endodermis; P, phloem tissue; T, transfusion tissue; X, xylem tissue.

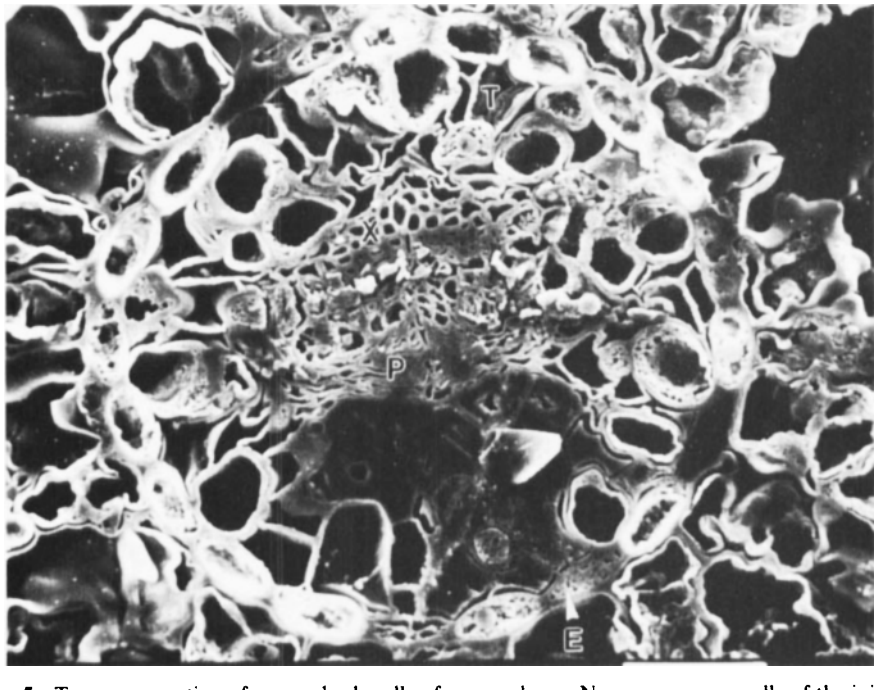

Figure 5 Transverse section of a vascular bundle of a second year Norway spruce needle of the injured forest site of Velmerstot (enlarged detail from identical needle of Figure 2). Bar = 50 μm. Explanations of abbreviations see legend of Figure 4.

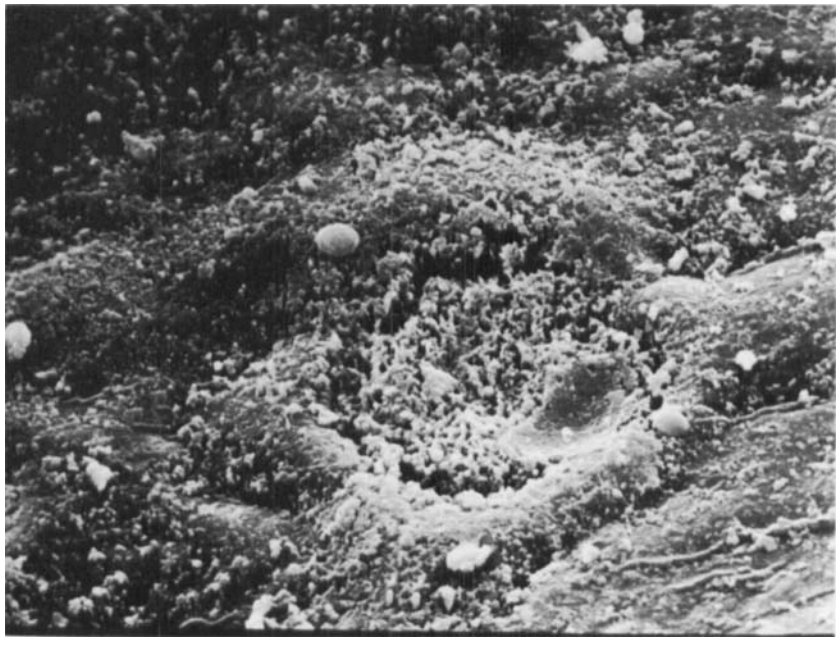

Figure 6 Surface area of a healthy second year Norway spruce needle (Glindfeld) with top view onto a stomate occluded with structural wax. Bar = 5 μm.

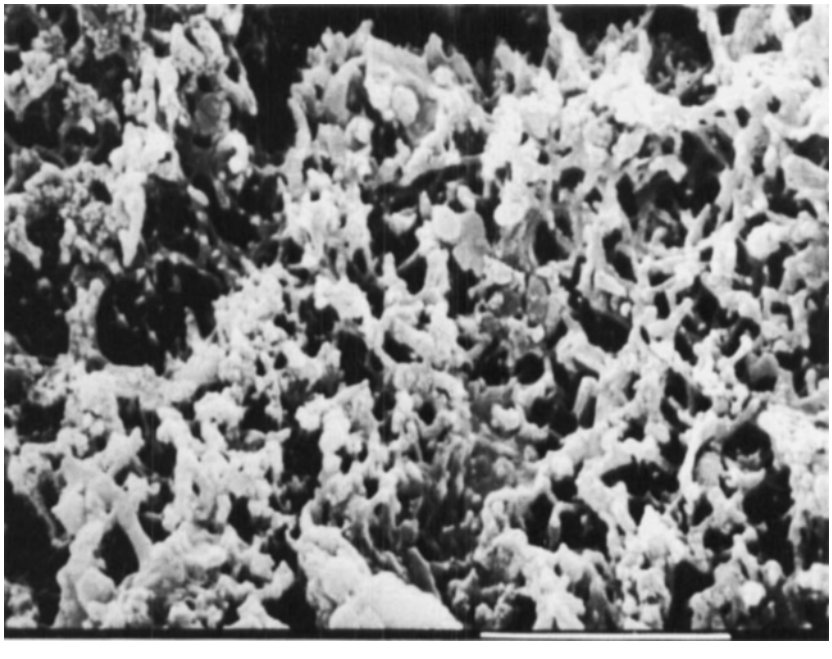

Figure 7 Wax rods of the epistomatal area (close-up from Figure 6). Bar = 5 μm.

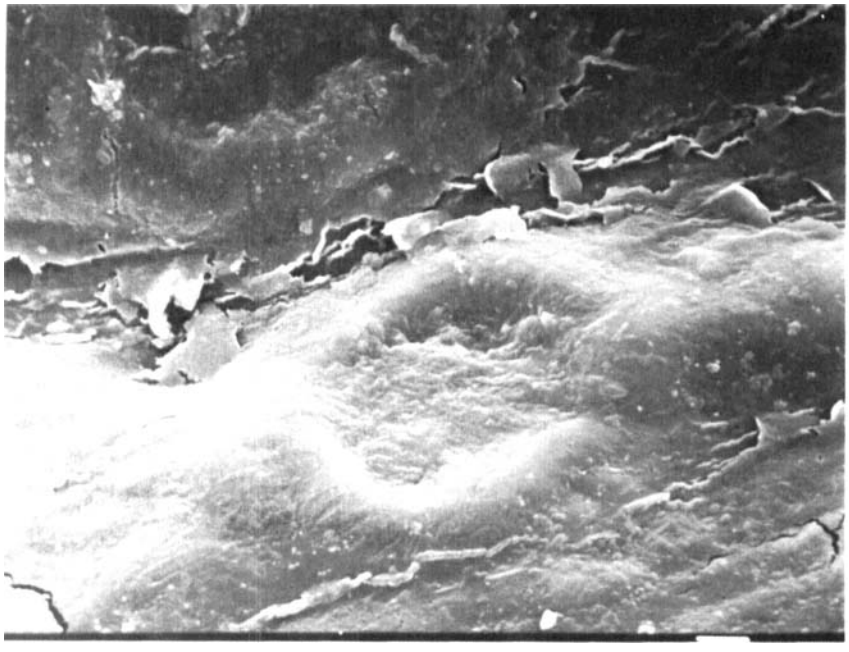

Figure 8 Surface area of an injured second year Norway spruce needle (Velmerstot) with top view onto a stomate occluded by a flattened wax plate. Cracks in the wax layer around the stomate are probably artefacts of preparation. Bar = 5 μm.

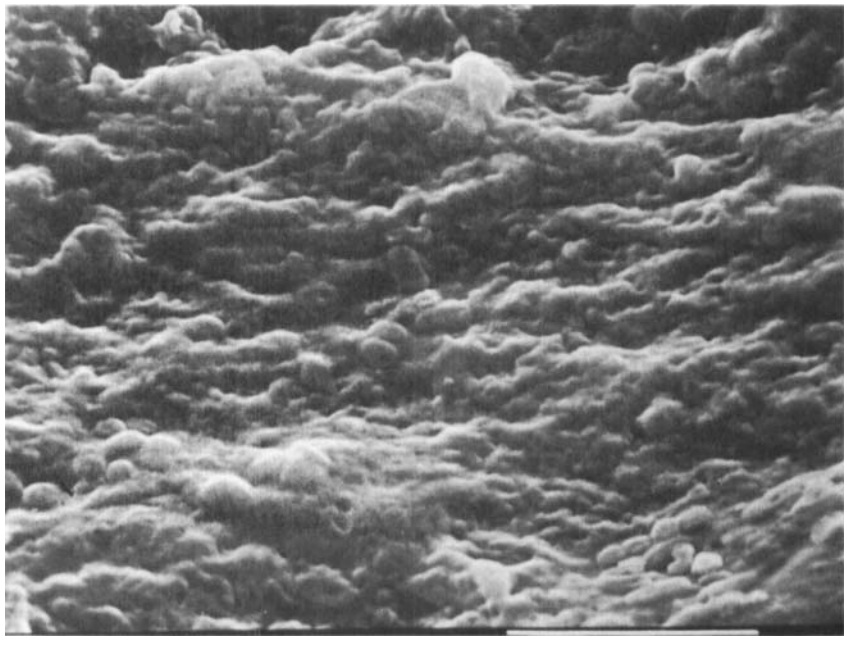

Figure 9 Flattened wax layer of the epistomatal area (close-up from Figure 8). Bar = 5 μm.

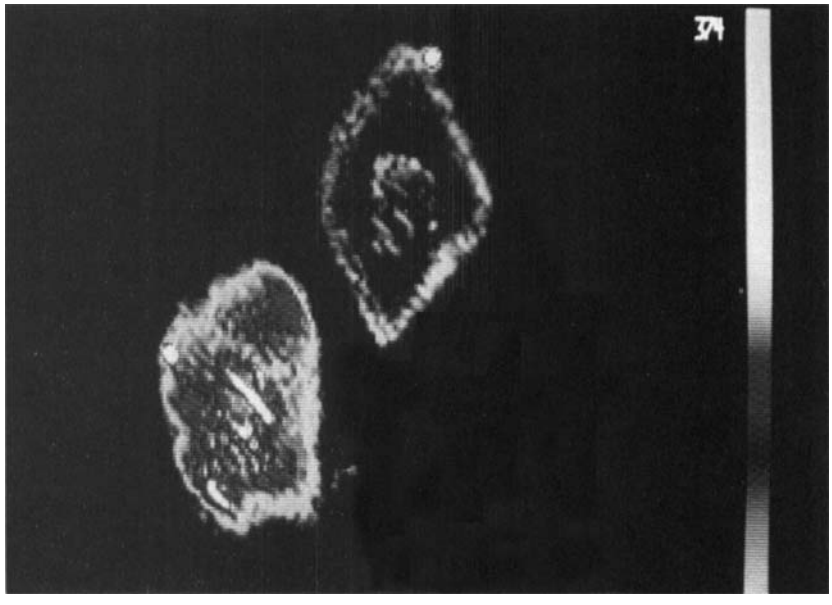

Figure 10 Transverse ^{1}H-NMR image of a healthy second year Norway spruce needle (site Glindfeld, upper right) and a damaged needle (site Velmerstot, lower left). Colours correlate with different ^{1}H levels (0–25% blue, 26–50% red, 51–100% yellow).

Figure 11 ^{1}H-NMR image of the same needles as in Figure 10, but in black and white contrast showing the apoplast pathways of the mesophyll tissues. The imaging delays were a TE of 7.4 ms and TR of 1 s. The in plane resolution is 11 μm, the slice thickness is 990 μm. 128 averages were taken for a 256*256 data array.

low a signal intensity as in the internal mesophyll tissue can be found in the epidermal and hypodermal layers.

Injured needles show another pattern of water distribution than do healthy needles. The most striking histological effect is the reversed distribution of water quantities in the mesophyll tissue. In contrast to the mesophyll of healthy needles, the internal part of mesophyll contains a higher signal intensity than the external part (Figure 10). Even higher signal intensities come from the endodermis and the xylem tissue showing a broad band of mobile water inside the vascular bundle (Figure 11). Free water is not homogeneously distributed in the mesophyll tissue. Patches of higher signal intensities alternate with areas of weak signal intensities. This may be due to the apoplast pathway of water, that is translocated through cell walls, and the intercellular air spaces.

More signals of mobile water can be detected in the mesophyll near the edges of the rhombic needle cross-cut; on the other hand there is a decreasing signal intensity in the centre of the peripheral side lines of the rhombic cross-cut (Figure 11). As can be seen in Figures 1 and 2, these tissue parts are the histological sites where the rows of stomates are located and loss of water vapour is facilitated by transpiration.

Discussion

Non-destructive measurement of relative water contents in living plant tissues is a promising tool to discriminate sensitively between healthy and diseased tissues. Pulsed NMR techniques compare favourably with other methods of measuring the moisture content of wood.

Several authors have reported on ^{1}H-NMR sub-millimetre-imaging of plant tissues[17,18] and even on an in-plane resolution of a few plant cells[19]. This is due to the use of high magnetic field strength. The qualitative distinction between water concentration and water binding in different tissue cells can be achieved by additional variation of the spin-echo time[19]. The reversed distribution of water quantities in the mesophyll tissue points to a disturbed water balance in the needles of the Velmerstot area.

This finding opens a new way for interpreting some damage symptoms, such as e.g. the formation of a thin and compact wax layer covering the needle surface and the epistomatal chambers and reduced evapotranspiration of damaged needles. As has been reported in an earlier paper[20], spruce needles of samples exposed to O_3 or SO_2, either separately or simultaneously, and spruce needles of a severely damaged field site in the Fichtelgebirge (NE-Bavaria, Germany) exhibited reduction of transpiration. At noon stress time, reference trees achieved remarkably higher maximum rates of transpiration than the damaged trees[20]. The same results were reported by Lange who found that damaged spruce twigs of an experimental site in the Fichtelgebirge exhibit a lower rate of transpiration and lower photosynthetic capacity[21]. The transpiration rate at the declining site of the Fichtelgebirge was 17.5% lower than

at the healthy site in 1986, though the declining site received 4% more rain and 12% more throughfall[22].

The water potential, ψ, of tissues can be described as the sum of the pressure potential, P, and the osmotic potential, π. As illustrated by the classical Höfler diagram the water potential slows down with increasing relative water content of tissues[23,24].

One consequence of a reduced water loss by transpiration is a decreased water flux through tracheids and sieve tubes. The latter are more collapsed in severely polluted sites than in healthy sites.

Pollution-induced changes in epicuticular waxes have been reported[25,26,27]. Healthy conifer needles exhibit fibrillar waxes in the epistomatal chamber. Structural degradation of fibrillar waxes into an amorphous wax type by air pollution plugs the whole stomatal chamber. This plugging has physiological consequences[28].

Higher amounts of water accumulate inside the needle and show reversed distribution in the mesophyll tissue. Damaged needles are thinner but longer. That is, the external surface significantly increases. This may be an adaptation for a shorter diffusion way to the sites of evapotranspiration.

CONCLUSIONS

^{1}H-NMR micro-imaging is a useful technique to discriminate sensitively between healthy and diseased tissues of spruce needles. One advantage of ^{1}H-NMR micro-imaging in contrast to alternative measurements of the relative water content is the non-destructive analysis of living organs and tissues. The same specimens can be used for further investigation in the living state. The reversed patterns of quantitative water distribution in the mesophyll tissue of healthy and injured spruce needles give rise to an early detection of tree decline. No other method of measuring water content is able to give information about quantitative water distribution in living tissues without damaging the specimens or exposing the living tissue to ionizing radiation.

The correlated investigations by ^{1}H-NMR micro-imaging, quantitative histological analysis, and scanning electron microscopy are a promising new approach to interpretation of forest decline symptoms.

References

1. P. C. Lauterbur, *Nature* (London) **242**, 190–191 (1973).
2. P. Mansfield and P. K. Grannel, *J. Phys. Chem.* **6**, 422–426 (1973).
3. C. D. Eccles and P. T. Callaghan, *J. Magn. Reson.* **68**, 393–398 (1986).
4. A. R. Sharp, M. T. Riggin, R. Kaiser and M. H. Schneider, *Wood and Fiber* **19**, 74–81 (1978).
5. C. D. Eccles, P. T. Callaghan, and C. F. Jenner, *Biophys. J.* **53**, 77–81 (1988).
6. P. T. Callaghan and C. D. Eccles, *J. Magn. Reson.* **71**, 426–445 (1987).
7. P. Schütt and E. B. Cowling, *Plant Disease* **69**, 548–558 (1985).
8. J. D. Barnes, D. Eamus and K. A. Brown, *New Phytol.* **114**, 713–720 (1990).
9. J. Hellkvist, G. P. Richards and P. G. Jarvis, *J. Applied Ecol.* **11**, 637–668 (1974).
10. K. Mengel, A. M. R. Hogrebe and A. Esch, *Physiol. Plant.* **75**, 201–207 (1989).
11. D. Eamus, J. Leith and D. Fowler, *Tree Physiol.* **5**, 387–397 (1989).
12. M. E. Ter-Pogossian, M. E. Raichle and B. E. Sobel, *Sci. Amer.* **243**, 141–155 (Oct. 1980).

13. Landesanstalt für Immissionsschutz des Landes Nordrhein-Westfalen "Berichte über die Luftqualität in Nordrhein-Westfalen", TEMES Jahresbericht 1988, 1989.
14. Minister für Umwelt, Raumordnung und Landwirtschaften des Landes Nordrhein-Wesfalen "Forschungsberichte zum Forschungsprogramm des Landes Nordrhein-Westfalen: Luftverunreinigung und Waldschäden" **1**, 211–238, (1987).
15. W. A. Edelstein, J. M. S. Hutchison, G. Johnson and T. Rudolph, *Phys. Med. Biol.* **25**, 751 (1980).
16. G. Masuch, H. G. Kicinski, A. Kettrup and K.-S. Boos, *Intern. J. Environ. Anal. Chem.* **32**, 187–212 (1988).
17. A. Connelly, J. A. B. Lohmann, B. C. Loughman, H. Quinquampoix and R. G. Ratcliffe, *J. Exp. Bot.* **38**, 1713–1723 (1987).
18. G. A. Johnson, J. Brown and P. J. Kramer, *Proc. Natl. Acad. Sci. USA* **84**, 2752–2755 (1987).
19. L. Walter, A. Balling, U. Zimmermann, A. Haase and W. Kuhn, *Planta* **178**, 524–530 (1989).
20. K. Vogels, R. Guderian and G. Masuch, *Studies in Environmental Science* **30**, 171–186 (1986).
21. O. L. Lange, *Allg. Forst Zeitschr.* **3**, 55–64 (1989).
22. E. D. Schulze, R. Hantschel, K. S. Werk, and R. Horn, in: E. D. Schulze, O. L. Lange, R. Oren (eds). 'Forest Decline and Air Pollution', Springer, Berlin 1989, p. 341–351.
23. E. W. R. Barlow, in: Dale, J. E., Milthorpe, F. L. (eds.) 'The Growth and Functioning of Leaves', London, 1983, p. 315–345.
24. M. Tesche, S. Feiler, G. Michael, H. Ranft, and Ch. Bellmann, *Eur. J. For. Path.* **19**, 281–292 (1989).
25. S. Huttunen and K. Laine, *Ann. Bot. Fennici* **20**, 79–86 (1983).
26. C. Rinallo, P. Raddi, R. Gellini and V. Di Leonardo, *Eur. J. For. Path.* **16**, 440–446 (1986).
27. T. Euteneuer, L. Steubing and R. Debus, *Angew. Botanik* **62**, 63–72 (1988).
28. J. J. Sauter and J. V. Voss, *Eur. J. For. Path.* **16**, 408–423 (1986).